Estimation of genetic variability and identification of regions under selection based on runs of homozygosity in Beijing-You Chickens

Hailong Wang,[1] Qiao Wang,[1] Xiaodong Tan, Jie Wang [ORCID], Jin Zhang, Maiqing Zheng, Guiping Zhao, and Jie Wen[2]

Chinese Academy of Agricultural Science, State Key Laboratory of Animal Nutrition, Beijing 100193, China

ABSTRACT The genetic composition of populations is the result of a long-term process of selection and adaptation to specific environments and ecosystems. Runs of homozygosity (**ROHs**) are homozygous segments of the genome where the 2 haplotypes inherited from the parents are identical. The detection of ROH can be used to describe the genetic variability and quantify the level of inbreeding in an individual. Here, we investigated the occurrence and distribution of ROHs in 40 Beijing-You Chickens from the random breeding population (BJY_C) and 40 Beijing-You Chickens from the intramuscular fat (**IMF**) selection population (BJY_S). Principal component analysis (**PCA**) and maximum likelihood (**ML**) analyses showed that BJY_C was completely separated from the BJY_S. The nucleotide diversity of BJY_C was higher than that of BJY_S, and the decay rate of LD of BJY_C was faster. The ROHs were identified for a total of 7,101 in BJY_C and 9,273 in BJY_S, respectively. The ROH-based inbreeding estimate (F_{ROH}) of BJY_C was 0.079, which was significantly lower than that of BJY_S ($F_{ROH} = 0.114$). The results were the same as the estimates of the inbreeding coefficients calculated based on homozygosity (F_{HOM}), the correlation between uniting gametes (F_{UNI}), and the genomic relationship matrix (F_{GRM}). Additionally, the distribution and number of ROH islands in chromosomes of BJY_C and BJY_S were significantly different. The ROH islands of BJY_S that included genes associated with lipid metabolism and fat deposition, such as *CIDEA* and *S1PR1*, were absent in BJY_C. However, *GPR161* was detected in both populations, which is a candidate gene for the formation of the unique five-finger trait in Beijing-You chickens. Our findings contributed to the understanding of the genetic diversity of random or artificially selected populations, and allowed the accurate monitoring of population inbreeding using genomic information, as well as the detection of genomic regions that affect traits under selection.

Key words: biodiversity, ROH, selection signature, chickens

INTRODUCTION

Common metrics used to assess genetic diversity include nucleotide diversity, effective allele frequency, polymorphic information content, and genotypic heterozygosity (Liu et al., 2020). The value of heterozygosity reflects the level of variation in the population and usually ranges between 0 and 1 (Madilindi et al., 2020). Higher heterozygosity represents richer genetic diversity (Kaviriri et al., 2020). Natural populations usually showed the large heterogeneities and high genetic diversities (Hoban et al., 2020). It was found that sheep populations deviated from Hardy-Weinberg equilibrium when the actual heterozygosity was lower than desired heterozygosity, suggesting the occurrence of selection or inbreeding (Windig et al., 2019). In addition, the most direct indicator for assessing the genetic diversity of a population is the inbreeding coefficient (Kalashnikov et al., 2020). Due to the rapid development of sequencing technologies, the use of resequencing data to calculate the true inbreeding coefficients of genomes is gradually becoming a trend.

The run of homozygosity (**ROH**) information can be used as an analytical indicator to better study the genetic diversity of livestock populations (Meyermans et al., 2020). In addition, common ancestry analyses based on ROHs can provide a more effective means of reducing inbreeding decline in breeding programs (Zhang et al., 2015). A previous study reported a

10-yr genetic diversity analysis of 3 local varieties in China, which revealed differences in genetic diversity after a long period of conservation efforts (Talebi et al., 2020). Research (Kim et al., 2013) on Holstein cows found that the distribution of ROHs on chromosomes provided a better understanding of genomic changes in selected regions. Populations that have selected specific traits exhibit reduced genetic diversity and changes in their ROH distributions throughout the genome (Szmatoła et al., 2019). Select regions throughout the whole genome are more likely to produce islands of ROH, which have lower genetic diversity and higher purity compared to other regions of the genome. The distribution of the ROH of genomic regions following selection was also determined in Arabian horses (Grilz-Seger et al., 2019) and in pigs (Bosse et al., 2012).

Beijing-You chicken is a local chicken breed in China, which is famous for its excellent meat and egg quality and unique appearance. In this study, we aimed to use a dense panel of single nucleotide polymorphisms to describe the genetic variability of Beijing-You Chickens, reveal their underlying population structure, and identify selection signatures by ROH. Comparisons between the inbreeding levels of conserved and selected populations of Beijing-You Chickens were performed and revealed genes responsible for adaptive variation in the selected population.

MATERIALS AND METHODS

Ethics Statement

The animal experiments were carried out in accordance with the Guidelines for Experimental Animals established by the Ministry of Science and Technology (Beijing, China). The study was approved by the Animal Management Committee of the Institute of Animal Sciences, Chinese Academy of Agricultural Sciences (Beijing, China). Ethical approval regarding animal survival was given by the animal ethics committee of IAS-CAAS (approval number: IASCAAS-AE20140615).

Animals and Sample Collection

Blood samples were collected from forty 120-day-old Beijing-You Chickens (17 males and 23 females) of a random breeding population (**BJY_C**) and 40 Beijing-You Chickens (22 males and 18 females) of a selection population (**BJY_S**) for DNA extraction. The BJY_S population was selected for the relative content of intramuscular fat for 5 yr, and 40 males were selected each year to be matched with 160 females.

Whole-Genome Resequencing

Blood collected from the veins of all animals was extracted using the standard phenol/chloroform extraction method. The quantity and quality of DNA extracted from whole blood samples were determined using a Nanodrop ND-1000 Spectrophotometer (Thermo Fisher Scientific Inc., Waltham, MA) and agarose gel electrophoresis was used to visually assess DNA integrity. Samples that passed the quality test were sent to the Beijing Compass Biotechnology Company for 10G whole-genome sequencing.

After sequencing, paired-end libraries were generated for each eligible sample using standard procedures. The average insert size was 300 to 500 bp, and the average read length was PE150 bp (150 bp paired-end reads). All libraries were separately sequenced on a HiSeq X Ten sequencer to average raw read sequence coverage of 10×.

The filtered raw reads were compared to the reference genome (version: ftp://ftp.ensembl.org/pub/release-101/fasta/gallus_gallus/dna/) using the MEM mode of BWA software (version 0.7.12). Picard (version 1.119) and SAMtools (version 1.9) were used to obtain the sorted BAM files. Before detecting mutations, the basic quality score recalibration (**BQSR**) was recalibrated, which involved 2 steps. In the first step, Base Recalibrator, the Picard tool and stool were used to obtain the classified BAM file for analysis. In the second step, Apply BQSR, the calibration table file obtained in the first step was used to readjust the basic quality value in the original BAM file. The new quality value was then re-exported to a new BAM file. GATK (version 4.0.2.1) was used to select GATK variants for filtering (Poplin, et al., 2018). The hard filter standards used for single nucleotide polymorphisms (**SNPs**) were QualByDepth (**QD**) < 2.0, RMSMappingQuality (**MQ**) < 40, FisherStrand (**FS**) > 60.0, StrandOddsRatio (**SOR**) > 3.0, and MappingQualityRankSumTest (**MQNankSum**) < −12.5.

The data were first filled with Beagle v5.0 software We first filled SNP genotypes with Beagle v5.0 (Ayres et al., 2012) for all SNP loci, and the filled SNP locus was quality-controlled using the Plink v1.9 software and then quality-controlled the SNPs using Plink v1.9 (Purcell et al., 2007), according to the following criteria: 1) the call rate was higher than 0.9; 2) the minor allele frequency (**MAF**) was higher than 0.05; and 3) SNPs were filtered to exclude loci assigned to unmapped contigs and sex chromosomes. After quality control, 80 chickens and 6,252,214 variants were retained. The clean DNA sequencing data reported in this paper have been deposited in the Genome Sequence Archive (Wang et al., 2017) in the BIG Data Center (2019) under accession number CRA004519, and can be publicly accessed at http://bigd.big.ac.cn/gsa.

Genetic Characterization

Different approaches and software were used to disclose the genetic structure of Beijing-You Chickens:

a) Wright's statistics, including observed heterozygosity (H_O), expected heterozygosity (H_E), and inbreeding coefficients. Genomic inbreeding based on homozygous SNPs was determined using PLINK v1.9 software. The inbreeding coefficient for an individual

(F_{HOM}) was computed as $F_{HOM} = (O - E)/(L - E)$, where O is the number of observed homozygotes, E is the number of homozygotes expected by chance, and L is the number of genotyped autosomal SNPs. Genomic SNP-by-SNP inbreeding coefficient (F_{GRM}) estimates were calculated using GCTA software. The F_{GRM} was calculated as $F_{GRM} = \frac{1}{m} \sum_{i=1}^{N} \left(\frac{[x_i - E(x_i)]^2}{2p_i(1-o_i)} - 1 \right)$, where x_i is the number of copies of the reference allele for the ith SNP, m is the number of SNPs, and p_i is the frequency of the reference allele. Genomic inbreeding coefficients were also estimated based on ROHs (F_{ROH}). The F_{ROH} for each animal was calculated as $F_{ROH} = \frac{\sum_i L_{ROHi}}{L_{auto}}$, where L_{ROHi} is the length of ROH_i of individual I, and L_{auto} is the autosomal genome length covered by the SNPs included on the chip. Genomic inbreeding coefficients were estimated based on uniting gametes (F_{UNI}). The F_{UNI} for each animal was calculated as $F_{UNI} = \frac{x_1^2 - 1 + 2p_i x_i + 2p_i^2}{2p_i(1-p_i)}$, where x_i is the number of copies of the reference allele for the ith SNP, and p_i is the frequency of the reference allele.

b) Linkage disequilibrium within 500 kb was calculated using PopLDdecay software (Zhang et al., 2019), and then, the genome-wide LD distribution was mapped based on marker spacing and r^2 values.

c) Principal component analyses (**PCA**) were performed using GCTA 64 software. The PCA of pairwise individual genetic distances was performed based on the allele frequencies of pruned SNPs.

d) ADMIXTURE v.1.3.0 software was used to infer the most probable number of ancestral populations based on the SNP data (Alexander et al., 2009). ADMIXTURE was run from K = 1 to K = 12, and the optimal number of clusters (K-value) was determined as the one having the lowest cross-validation error. Each inferred chicken population structure was visualized using an R script, as suggested in the ADMIXTURE procedure.

e) A maximum likelihood (**ML**) tree was created and graphically represented using RAxML and FigTree version 1.4.2 (http://tree.bio.ed.ac.uk/software/figtree) software, respectively.

f) ROH analysis was performed for each individual (complete SNP dataset = 6,252,214) using Plink software. The ROH was defined by (Yuan, et al., 2022): 1) a minimum of 200 kb in size and 100 homozygous SNPs; 2) one heterozygous SNP was permitted in the ROH, so that the length of the ROH was not disrupted by an occasional heterozygote; 3) one missing SNP was allowed in the ROH; 4) the maximum gap between SNPs of 40 kb was predefined to ensure that the SNP density did not affect the ROH. According to the nomenclature reported by other authors (Zavarez, et al., 2015), the ROHs were grouped into 5 classes of length: <0.5 Mb, 0.5-0.1 Mb, 1-2 Mb, 2-4 Mb, and >4 Mb. Number, total length, and the average ROH length were calculated across individuals within the chicken populations. In addition, the percentage of the total genome length affected by the ROH was also estimated.

RESULTS

Genetic Diversity Analysis

A comparison of the nucleotide polymorphisms of the 2 populations revealed that the nucleotide diversity (**Pi**) of BJY_C (0.0027) was slightly higher than that of BJY_S (0.0025) (Table 1). The observed heterozygosity (H_O) and expected heterozygosity (H_E) of BJY_C (H_O = 30.26%, H_E = 31.48%) were significantly higher than that of BJY_S (H_O = 26.19%, H_E = 29.51%), and the difference between the H_O and H_E of BJY_S (3.31%) was higher than that of BJY_C (1.22%) (Table 1). In addition, the mean inbreeding coefficient of BJY_C (F_{HOM} = 0.0605, F_{GRM} = 0.0662, F_{UNI} = 0.0637, F_{ROH} = 0.079) was significantly lower than that of BJY_S (F_{HOM} = 0.1868, F_{GRM} = 0.1384, F_{UNI} = 0.1646, F_{ROH} = 0.114) (Table 1).

Genetic Characterization

The degree of LD was attenuated with increasing marker distance, and the decay rate of LD was also decreased gradually. The LD decay analysis showed that BJY_C had a faster decay rate of LD than that of BJY_S (Figure 1). In the PCA analysis, BJY_C was completely separated from the BJY_S, and there were no outlying samples (Figure 2A).

The ADMIXTURE program was run for K values from 2 to 3 (Figure 2B and 2D). The lowest cross validation error was found at K = 2, and represents the number of ancestors in Beijing-You Chickens (Figure 2C). A number

Table 1. Genetic diversity analysis in BJY_C and BJY_S.

	Pi	H_O	H_E	F_{HOM}	F_{GRM}	F_{UNI}	F_{ROH}
BJY_C	0.002717	0.302681	0.314877	0.0605	0.0662	0.0637	0.079
BJY_S	0.002552	0.261985	0.295136	0.1868	0.1384	0.1646	0.114

Note: BJY_C and BJY_S represent a random breeding population of Beijing-You Chickens and a selection population of Beijing-You Chickens based on intramuscular fat, respectively. Pi, H_O and H_E represent the nucleotide diversity, heterozygosity, and heterozygosity, respectively. F_{HOM} represents the inbreeding coefficient for an individual, F_{GRM} represents the genomic SNP-by-SNP inbreeding coefficient, and F_{UNI} and F_{ROH} represent the genomic inbreeding estimates based on the correlation between uniting gametes and ROHs, respectively.
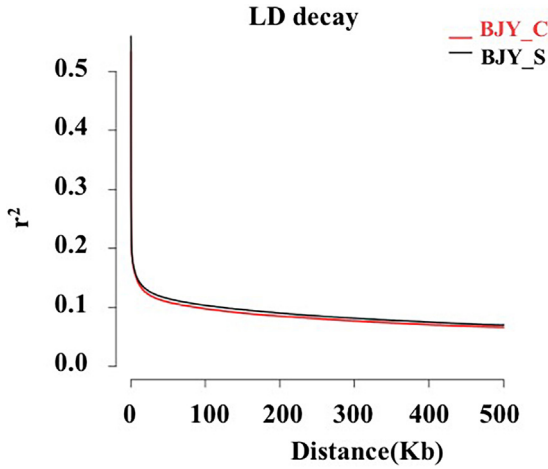
Figure 1. LD decay analysis in BJY_C and BJY_S. LD decay map measured by the r^2 over the distance between SNPs in the two Beijing-You Chicken populations. BJY_C and BJY_S represent a random breeding population and a selection population of Beijing-You Chickens based on intramuscular fat, respectively. Abbreviation: SNPs, single nucleotide polymorphisms.

of K greater than 2 did not produce a larger number of ancestor contributions in Beijing-You Chickens, as is shown in Figure 2B and 2D. When K = 2, the samples had the best segregation (Figure 2B) as the cross-validation result was the lowest (Figure 2C), and segregation occurred between BJY_C and BJY_S. A phylogenetic tree for BJY_C and BJY_S was constructed using probabilistic methods of phylogenetic inference (Figure 3). All the samples of BJY_C were clustered together, as did the samples of BJY_S, with no outliers.
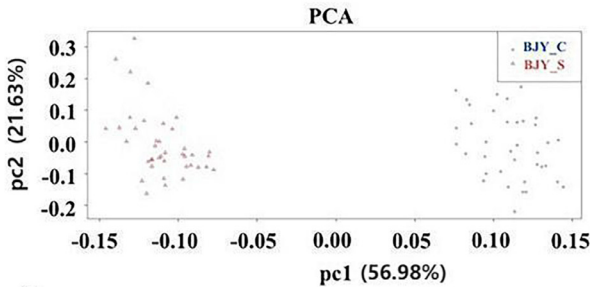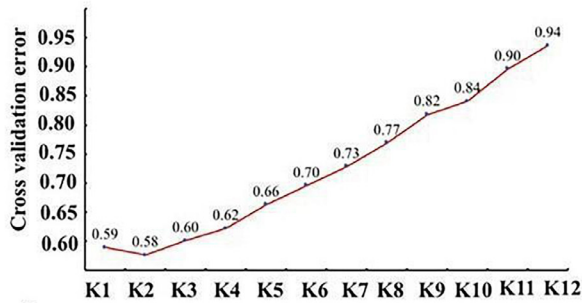
Summary of Runs of Homozygosity

The total number of ROHs detected on all chromosomes is shown in Tables 2 and 3. A total of 7,101 runs in BJY_C (Table 2) and 9,273 runs in BJY_S (Table 3) were identified. The results showed that the number of ROHs in BJY_S increased by 2172 compared to BJY_C. The ROHs less than 0.5 Mb and 0.5−1 Mb accounted for a relatively high proportion of the total ROH in both populations (BJY_C: 76%, 20%, BJY_S: 70%, 23%, respectively). The results also showed that the percentage of the ROHs less than 0.5 Mb of BJY_C was higher than that of BJY_S, but with lengths between 0.5 and 1 Mb was less. In addition, there were no ROHs with lengths greater than 4 Mb in BJY_C, but 2 were detected in the selected population, located on chromosomes 15 and 18, respectively. It is worth mentioning that we did not find any ROH on Chr31 in any of the 80 chickens.

Except for 2 chiekens in BJY_C, the average length of ROHs in other individuals was greater than 0.35 Mb in both populations, and the number of ROHs in most individuals ranged from 150 to 250. The lenth of most ROHs per individual ranged (as mean values) from 0.35 Mbp to 0.5 Mbp (Figure 4).

Functional Annotation of Genes

IMF in breast muscle (IMF_{br}, %) (dry weight basis) of BJY_S (BJY_S: $IMF_{br}= 2.85 \pm 0.90$) was significantly higher than that of BJY_C (BJY_C: $IMF_{br}= 2.60 \pm 0.78$, $P < 0.05$) due to the artificial selection (Liu et al.,
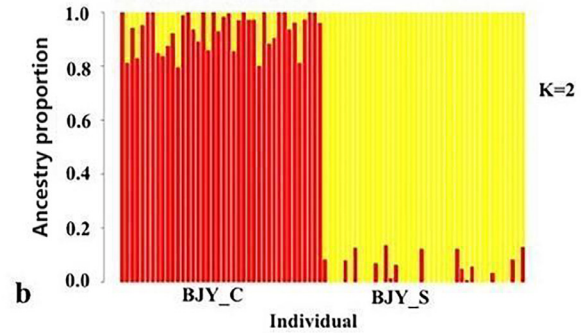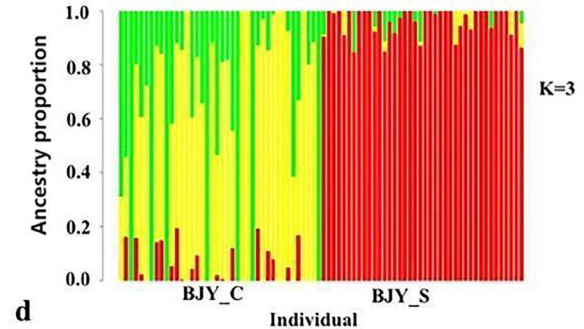
Figure 2. PCA and population structure analyses. (A) PCA in BJY_C and BJY_S. (B) Population structure analysis in BJY_C and BJY_S (K = 2). (C) Cross-validation results. (D) Population structure analysis in BJY_C and BJY_S (K = 3). BJY_C and BJY_S represent a random breeding population of Beijing-You Chickens and a selection population of Beijing-You Chickens based on intramuscular fat, respectively. Abbreviation: PCA, principal component analysis.
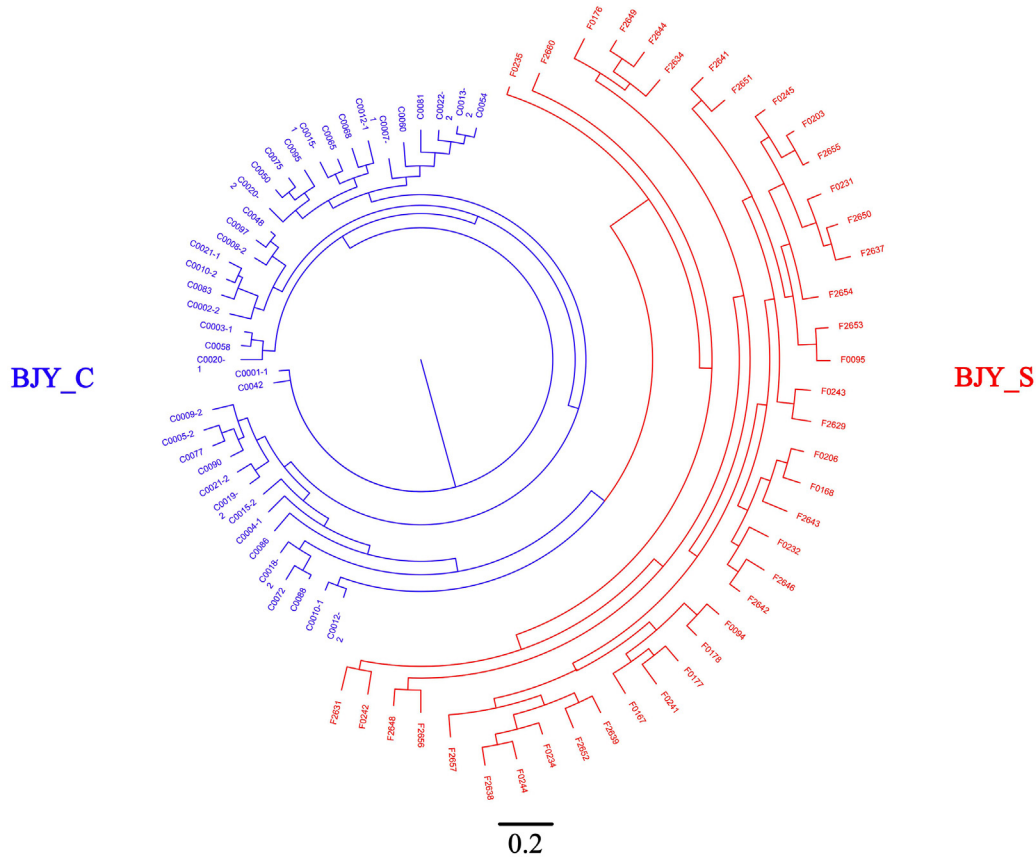
Figure 3. Phylogenetic tree for BJY_C and BJY_S. BJY_C and BJY_S represent a random breeding population of Beijing-You Chickens and a selection population of Beijing-You Chickens based on intramuscular fat, respectively.

2019). To identify candidate genes associated with the selected trait, the incidence of ROH fragments across the genome was presented as a Manhattan plot (Figure 5). The genomic distribution of ROH segments was non-uniform across chromosomes in BJY_C and BJY_S. The threshold used to define ROH islands was 37.5 and 47.5% in BJY_C and BJY_S, respectively. We selected the top 10 ROH islands in the top 1% of SNPs most commonly observed in the ROHs of the 2 populations. We annotated the associated genes based on the autosomal chicken gene list (Gallus_gallus. GRCg6a.101.gff3) (Tables 4 and 5). In BJY_C, there were seven genes in the ROH islands on chromosome 1, two genes on chromosomes 5 and 15, and one gene on chromosome 17. Additionally, there were 17 genes in ROH islands on chromosome 1, nine genes on chromosome 2, and eight genes on chromosome 8 in BJY_S. Multiple ROH islands were identified on chromosome 1 in both populations. Among them, 6 of the top ten ROH islands in BJY_S were located on chromosome 1, while 5 of the top 10 ROH islands were located on chromosome 1 in BJY_C. Three common genes, *GPR161, ST3GAL6* and *COL8A1*, were observed in multiple overlapping regions on chromosome 1 in both populations. Moreover, the ROH islands on chromosome 1 of BJY_S also harbored genes associated with lipid metabolism and fat deposition, such as *CIDEA* and *S1PR1*, however, such genes were absent in BJY_C.

DISCUSSION

In this study, the patterns of variation in high-density SNPs were used to detect genetic variability between conserved and selected populations of Beijing-You Chickens. Through ROH analyses of resequencing information, the findings of this study highlighted changes in the population structure and variant genes of Beijing-You Chickens.

Nucleotide diversity is a commonly used measure of diversity within or between populations, and is a quantitative indicator of genetic variation (Tatarinova et al., 2016; Adhikari et al., 2020). Nucleotide diversity is also often associated with other values that measure population diversity, such as the expected heterozygosity (Selvam et al., 2017; López-Cortegano et al., 2019). With the widespread use of SNP gene chips and resequencing technologies for livestock, ROH studies based on genomic information are becoming increasingly prevalent (Rodríguez-Ramilo et al., 2019). Population structure and population evolution studies based on ROHs have also been performed in cattle (Bos taurus) (Xu et al., 2019), pigs (Xie et al., 2019; Shi et al., 2020), horses (Grilz-Seger et al., 2019), sheep (Deniskova et al., 2019; Gorssen et al., 2020), goats (Nandolo et al., 2018), and chickens (Talebi, et al., 2020). Our results showed that BJY_S, with relatively homogeneous genetic diversity, had smaller Pi values compared to BJY_C. These

Table 2. Numbers of ROH per chromosome according to ROH classes of length in BJY_C.

Chr	<0.5 MB[1]	0.5−1 MB[1]	1−2 MB[1]	2−4 MB[1]	>4 MB[1]	Total
1	1,065 (0.8)	243 (0.18)	17 (0.01)	0 (0)	0 (0)	1,325
2	774 (0.83)	154 (0.16)	10 (0.01)	0 (0)	0 (0)	938
3	603 (0.78)	140 (0.18)	27 (0.04)	0 (0)	0 (0)	770
4	419 (0.79)	92 (0.17)	20 (0.04)	0 (0)	0 (0)	531
5	376 (0.75)	98 (0.2)	28 (0.06)	0 (0)	0 (0)	502
6	236 (0.73)	66 (0.2)	22 (0.07)	0 (0)	0 (0)	324
7	277 (0.72)	88 (0.23)	20 (0.05)	2 (0.01)	0 (0)	387
8	129 (0.69)	39 (0.21)	19 (0.1)	0 (0)	0 (0)	187
9	132 (0.69)	36 (0.19)	22 (0.11)	2 (0.01)	0 (0)	192
10	109 (0.59)	58 (0.32)	15 (0.08)	2 (0.01)	0 (0)	184
11	134 (0.62)	63 (0.29)	18 (0.08)	0 (0)	0 (0)	215
12	113 (0.7)	33 (0.2)	10 (0.06)	6 (0.04)	0 (0)	162
13	149 (0.73)	43 (0.21)	11 (0.05)	0 (0)	0 (0)	203
14	96 (0.72)	27 (0.2)	11 (0.08)	0 (0)	0 (0)	134
15	80 (0.57)	39 (0.28)	16 (0.11)	5 (0.04)	0 (0)	140
16	2 (1)	0 (0)	0 (0)	0 (0)	0 (0)	2
17	71 (0.65)	25 (0.23)	11 (0.1)	2 (0.02)	0 (0)	109
18	69 (0.62)	33 (0.3)	8 (0.07)	1 (0.01)	0 (0)	111
19	81 (0.71)	23 (0.2)	8 (0.07)	2 (0.02)	0 (0)	114
20	88 (0.63)	32 (0.23)	19 (0.14)	1 (0.01)	0 (0)	140
21	55 (0.71)	12 (0.15)	11 (0.14)	0 (0)	0 (0)	78
22	35 (0.92)	3 (0.08)	0 (0)	0 (0)	0 (0)	38
23	53 (0.82)	11 (0.17)	1 (0.02)	0 (0)	0 (0)	65
24	40 (0.78)	9 (0.18)	2 (0.04)	0 (0)	0 (0)	51
25	16 (1)	0 (0)	0 (0)	0 (0)	0 (0)	16
26	40 (0.8)	8 (0.16)	2 (0.04)	0 (0)	0 (0)	50
27	43 (0.88)	6 (0.12)	0 (0)	0 (0)	0 (0)	49
28	38 (0.9)	3 (0.07)	1 (0.02)	0 (0)	0 (0)	42
30	3 (1)	0 (0)	0 (0)	0 (0)	0 (0)	3
31	0	0	0	0	0	0
32	3 (1)	0 (0)	0 (0)	0 (0)	0 (0)	3
33	34 (0.94)	2 (0.06)	0 (0)	0 (0)	0 (0)	36

[1]Proportion calculated as number of ROH per class over the total number of ROH.

Table 3. Numbers of ROH per chromosome according to ROH classes of length in BJY_S.

Chr	<0.5 MB[1]	0.5−1 MB[1]	1−2 MB[1]	2−4 MB[1]	>4 MB[1]	Total
1	1,440 (0.74)	462 (0.24)	42 (0.02)	0 (0)	0 (0)	1,944
2	1,024 (0.78)	249 (0.19)	33 (0.03)	0 (0)	0 (0)	1,306
3	819 (0.76)	211 (0.2)	44 (0.04)	1 (0)	0 (0)	1,075
4	496 (0.71)	150 (0.22)	46 (0.07)	2 (0)	0 (0)	694
5	411 (0.67)	152 (0.25)	45 (0.07)	1 (0)	0 (0)	609
6	259 (0.64)	117 (0.29)	29 (0.07)	0 (0)	0 (0)	405
7	234 (0.61)	104 (0.27)	43 (0.11)	4 (0.01)	0 (0)	385
8	185 (0.66)	63 (0.23)	30 (0.11)	1 (0)	0 (0)	279
9	198 (0.67)	70 (0.24)	26 (0.09)	3 (0.01)	0 (0)	297
10	89 (0.52)	52 (0.3)	27 (0.16)	3 (0.02)	0 (0)	171
11	113 (0.53)	75 (0.35)	23 (0.11)	3 (0.01)	0 (0)	214
12	141 (0.62)	54 (0.24)	30 (0.13)	1 (0)	0 (0)	226
13	136 (0.63)	53 (0.25)	25 (0.12)	1 (0)	0 (0)	215
14	108 (0.54)	59 (0.3)	29 (0.15)	3 (0.02)	0 (0)	199
15	84 (0.54)	38 (0.25)	23 (0.15)	9 (0.06)	1 (0.01)	155
16	2 (1)	0 (0)	0 (0)	0 (0)	0 (0)	2
17	79 (0.6)	33 (0.25)	16 (0.12)	4 (0.03)	0 (0)	132
18	73 (0.54)	39 (0.29)	18 (0.13)	5 (0.04)	1 (0.01)	136
19	97 (0.66)	31 (0.21)	17 (0.12)	2 (0.01)	0 (0)	147
20	101 (0.62)	31 (0.19)	19 (0.12)	13 (0.08)	0 (0)	164
21	41 (0.68)	18 (0.3)	1 (0.02)	0 (0)	0 (0)	60
22	37 (0.84)	7 (0.16)	0 (0)	0 (0)	0 (0)	44
23	59 (0.75)	13 (0.16)	7 (0.09)	0 (0)	0 (0)	79
24	53 (0.73)	12 (0.16)	6 (0.08)	2 (0.03)	0 (0)	73
25	22 (0.88)	3 (0.12)	0 (0)	0 (0)	0 (0)	25
26	40 (0.63)	17 (0.27)	5 (0.08)	1 (0.02)	0 (0)	63
27	57 (0.8)	12 (0.17)	2 (0.03)	0 (0)	0 (0)	71
28	48 (0.81)	9 (0.15)	2 (0.03)	0 (0)	0 (0)	59
30	9 (1)	0 (0)	0 (0)	0 (0)	0 (0)	9
31	0	0	0	0	0	0
32	2 (1)	0 (0)	0 (0)	0 (0)	0 (0)	2
33	31 (0.94)	2 (0.06)	0 (0)	0 (0)	0 (0)	33

[1]Proportion calculated as number of ROH per class over the total number of ROH.

findings were in agreement with the results of another study (Kijas et al., 2019) where selection led to a decrease in population diversity. The effective number of polymorphic SNPs (considered as the number of SNP in which at least one heterozygous individual was identified) represents the 99.9% of the total loci (Zhang et al., 2017). The moderately high values of H_O and H_E reflected the high percentage of polymorphic SNPs in BJY_C.

LD analysis showed that the LD decayed slower in the selected population than in the randomly conserved population of Beijing-You Chickens, and that the 2 populations could be clearly distinguished by PCA. ADMIXTURE analyses (Figure 2B) showed that when K = 2, all individuals were clearly divided into 2 subpopulations, including red for BJY_C and yellow for BJY_S. It was also shown in the literature that ADMIXTURE analyses determined that no excess occurred between the two populations, which is also consistent with the 2 populations in this study (Yang et al., 2019; Smaragdov and Kudinov, 2020). Thus, the collective results of this study indicated that the genetic backgrounds of the 2 populations of Beijing-You Chickens were different.

Traditionally, the inbreeding coefficient is estimated using pedigree data (F_{PED}). However, F_{PED} could not completely reveal the relatedness among individuals in the population, especially the missing parent or incorrect parent information. With the development of high-throughput genotyping technologies, genomic inbreeding coefficients, such as F_{ROH}, F_{HOM}, F_{UNI}, and F_{GRM} can be computed using molecular information. In fact, the inbreeding coefficients calculated using different
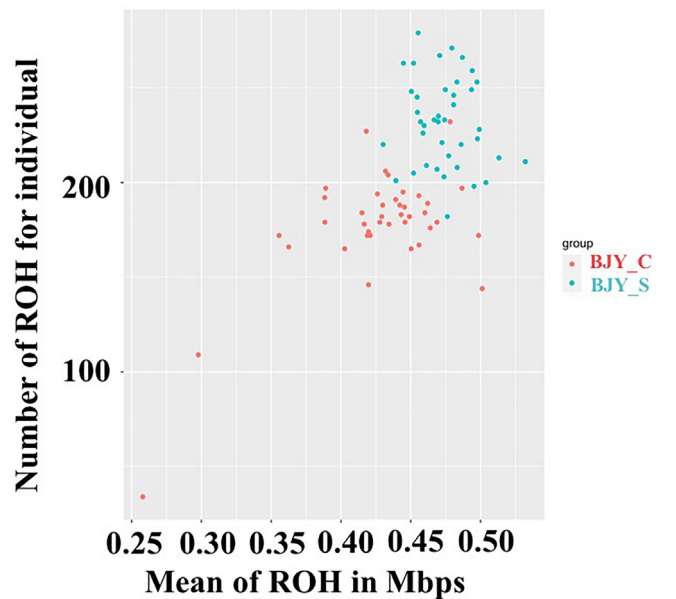

Figure 4. Relationship between the number and average length of ROHs in each individual in BJY_C and BJY_S. BJY_C and BJY_S represent a random breeding population of Beijing-You Chickens and a selection population of Beijing-You Chickens based on intramuscular fat, respectively. Abbreviation: ROHs, runs of homozygosity.
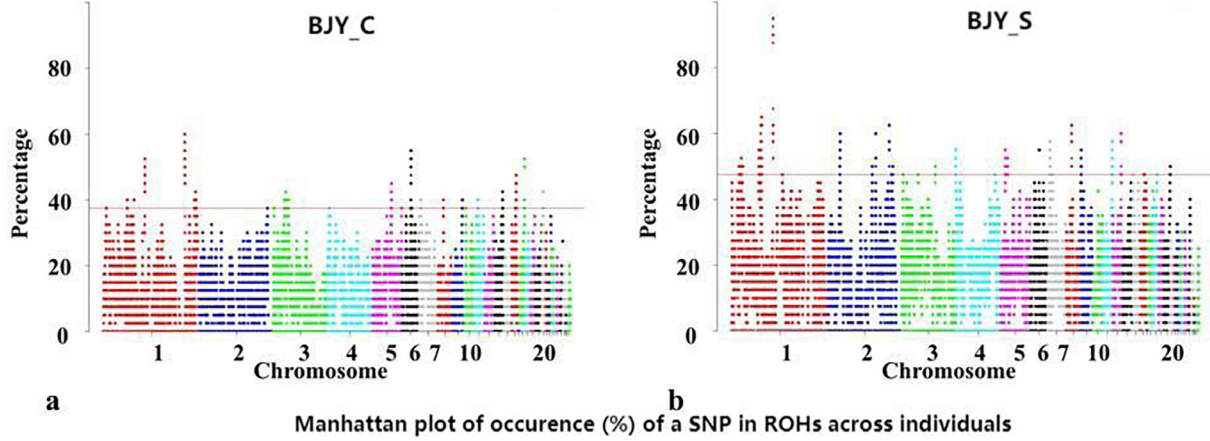
Figure 5. (A) The incidence of SNPs in the ROHs identified by PLINK in BJY_C samples. The red line indicates the adopted threshold: top 1% of all observations; (B) the incidence of SNPs in the ROHs identified by PLINK in BJY_S samples. The red line indicates the adopted threshold: top 1% of all observations. BJY_C and BJY_S represent a random breeding population of Beijing-You Chickens and a selection population of Beijing-You Chickens based on intramuscular fat, respectively. Abbreviations: ROHs, runs of homozygosity; SNPs, single nucleotide polymorphisms.

methods in different buffalo populations were similar, and all were representative of inbreeding (Ghoreishifar et al., 2020). F_{HOM} may overestimate inbreeding levels because it cannot distinguish IBD alleles from IBS alleles (Wang et al., 2014). In addition, F_{HOM} and F_{GRM} values can be negative for some individuals. Thus, F_{ROH} may be a more accurate method for quantifying animal inbreeding levels, which can alleviate the issues mentioned above (Liu et al., 2020). Also, the report showed that there were clear variations in the inbreeding of ROH arising from the selection pressure experienced by the chickens (Zhang et al., 2020). In this study, we calculated the different genomic inbreeding coefficients of BJY_S and BJY_C. The F_{HOM}, F_{UNI}, F_{GRM}, and F_{ROH} showed the same results, that the inbreeding coefficient of BJY_S was higher than that of BJY_C. Additionally, the F_{HOM}, F_{UNI}, F_{GRM}, and F_{ROH} were similar in the BJY_C population, while F_{HOM} was the highest (0.1868) and F_{ROH} was the lowest (0.114) in the BJY_S population.

Table 4. The 10 top 1% ROH identified on BJY_C autosomes by PLINK.

ROH_ID	Chr	Start	End	Length	Genes
S1	1	166960573	167004023	43.451	*
S2	6	19191553	19303357	111.805	*
S3	1	85255139	85300605	45.467	GPR161
S4	1	85300979	85461940	160.962	ST3GAL6, COL8A1
S5	17	10341476	10589614	248.139	ALC, LMX1B, ZBTB43, ZBTB34, RALGPS1
S7	1	85536245	85555292	19.048	*
S8	1	85556811	85602505	45.695	*
S9	15	9478785	9515894	37.11	MLEC, CABP1
S10	5	39087143	39247885	160.743	ANGEL1, IRF2BPL

Note: The threshold of 1% is determined by the incidence of SNPs in ROH.

ROHs are not randomly distributed throughout the genome, and most ROHs appear in the selected regions, where they cluster as ROH islands. Compared to other regions of the genome, ROH islands have low genetic diversity and high homozygosity. Therefore, ROH islands contain many candidate genes related to specific traits (Zhang et al., 2018). We identified a large number of ROH islands in the BJY_S and BJY_C populations, and the number and distribution of which were significantly different. *GPR161, ST3GAL6*, and *COL8A1* were the common genes in the top 10 ROH islands of the 2 populations.

A previous study showed that GPR161, a G protein coupled receptor, negatively regulated the sonic hedgehog pathway (**SHH**) through cAMP signaling (Mukhopadhyay et al., 2013). SHH is involved in limb development in vertebrates (Lin et al., 2020), and is a candidate gene responsible for the polydactylous mouse mutant Sasquatch phenotype (Sharpe et al., 1999). Thus, *GPR161* may also be a candidate gene for the formation of the unique five-finger trait in Beijing-You chickens.

Some genes associated with lipid metabolism and fat deposition, such as *CIDEA* and *S1PR1*, were identified on the ROH islands of BJY_S, but were absent in BJY_C. *CIDEA* was identified to bind lipid droplets and regulate their enlargement, thereby restricting lipolysis and favoring lipid storage (Jash et al., 2019). Additionally, single-locus and multilocus genome-wide association studies for IMF in duroc pigs showed that *S1PR1* was associated with IMF based on its potential functional roles in lipid metabolism (Ding et al., 2019). The formation of these ROH islands with genes related to fat metabolism may be related to the artificial selection of IMF in Beijing-You chickens.

We used ROH to estimate the inbreeding coefficient in Beijing-You Chickens. The results showed that inbreeding was higher in the BJY_S (Table 1). We found significant differences in the total number of ROHs in individuals from the 2 different populations, and the

Table 5. The 10 top 1% ROH identified on BJY_S autosomes by PLINK.

ROH_ID	Chr	Start	End	Length	Genes
S1	1	85091987	85293268	201.282	XCL1, TBX19, SFT2D2, TIPRL, GPR161
S2	1	61752650	61935152	182.503	CECR2, ATP6V1E1, BCL2L13, BID, MICAL3
S3	1	60296423	60308004	11.582	B4GALNT3
S4	1	85345783	85349098	3.316	ST3GAL6
S5	1	85349296	85555275	205.98	ST3GAL6, COL8A1
S6	2	124484650	124687601	202.952	TMEM64, NECAB1, C8orf88, TMEM55A, OTUD6A
S7	8	12053394	12310353	256.96	S1PR1, DPH5, SLC30A7, EXTL2, CDC14A, GPR88, RTCA, DBT
S8	1	85556657	85659949	103.293	DCBLD2
S9	2	24252892	24312980	60.089	*
S10	2	97166796	97312472	145.677	SPIRE1, PRELID3A, AFG3L2, TUBB6, CIDEA, IMPA2, MPPE1

Note: The threshold of 1% is determined by the incidence of SNPs in ROH.

average length of ROHs was longer in BJY_S, thus, also suggesting that selection and a reduction in population size was more likely to form ROH. Those findings were also in agreement with the results of ROH studies in different breeds of cattle (Cendron, et al., 2021). ROH islands are subject to stress selection when the candidate genes in such regions undergo adaptive selection (Mastrangelo, et al., 2017), and thus, the candidate genes obtained in this study based on the ROH islands can be used to distinguish changes in genetic levels following selection in Beijing-You Chickens.

ACKNOWLEDGMENTS

DISCLOSURES

The authors declare no conflict of interest.

SUPPLEMENTARY MATERIALS

Supplementary material associated with this article can be found in the online version at doi:10.1016/j.psj.2022.102342.

REFERENCES

Database resources of the BIG data center in 2019. (2019). Nucleic Acids Res. 47:D8–d14.

Adhikari, P., E. Goodrich, S. B. Fernandes, A. E. Lipka, P. Tranel, P. Brown, and T. M. Jamann. 2020. Genetic variation associated with PPO-inhibiting herbicide tolerance in sorghum. PLoS One 15:e0233254.

Alexander, D. H., J. Novembre, and K. Lange. 2009. Fast model-based estimation of ancestry in unrelated individuals. Genome Res. 19:1655–1664.

Ayres, D. L., A. Darling, D. J. Zwickl, P. Beerli, M. T. Holder, P. O. Lewis, J. P. Huelsenbeck, F. Ronquist, D. L. Swofford, M. P. Cummings, A. Rambaut, and M. A. Suchard. 2012. BEAGLE: an application programming interface and high-performance computing library for statistical phylogenetics. Syst. Biol. 61:170–173.

Bosse, M., H. J. Megens, O. Madsen, Y. Paudel, L. A. Frantz, L. B. Schook, R. P. Crooijmans, and M. A. Groenen. 2012. Regions of homozygosity in the porcine genome: consequence of demography and the recombination landscape. PLos Genet. 8:e1003100.

Cendron, F., S. Mastrangelo, M. Tolone, F. Perini, E. Lasagna, and M. Cassandro. 2021. Genome-wide analysis reveals the patterns of genetic diversity and population structure of 8 Italian local chicken breeds. Poult. Sci. 100:441–451.

Deniskova, T., A. Dotsev, E. Lushihina, A. Shakhin, E. Kunz, I. Medugorac, H. Reyer, K. Wimmers, N. Khayatzadeh, J. Sölkner, A. Sermyagin, A. Zhunushev, G. Brem, and N. Zinovieva. 2019. Population structure and genetic diversity of sheep breeds in the Kyrgyzstan. Front. Genet. 10:1311.

Ding, R., M. Yang, J. Quan, S. Li, Z. Zhuang, S. Zhou, E. Zheng, L. Hong, Z. Li, G. Cai, W. Huang, Z. Wu, and J. Yang. 2019. Single-locus and multi-locus genome-wide association studies for intramuscular fat in duroc pigs. Front. Genet. 10:619.

Ghoreishifar, S. M., H. Moradi-Shahrbabak, M. H. Fallahi, A. Jalil Sarghale, M. Moradi-Shahrbabak, R. Abdollahi-Arpanahi, and M. Khansefid. 2020. Genomic measures of inbreeding coefficients and genome-wide scan for runs of homozygosity islands in Iranian river buffalo, Bubalus bubalis. BMC Genet. 21:16.

Gorssen, W., R. Meyermans, N. Buys, and S. Janssens. 2020. SNP genotypes reveal breed substructure, selection signatures and highly inbred regions in Piétrain pigs. Anim. Genet. 51:32–42.

Grilz-Seger, G., T. Druml, M. Neuditschko, M. Mesarič, M. Cotman, and G. Brem. 2019. Analysis of ROH patterns in the Noriker horse breed reveals signatures of selection for coat color and body size. Anim. Genet. 50:334–346.

Hoban, D. B., S. Shrigley, B. Mattsson, L. S. Breger, U. Jarl, T. Cardoso, J. Nelander Wahlestedt, K. C. Luk, A. Björklund, and M. Parmar. 2020. Impact of α-synuclein pathology on transplanted hESC-derived dopaminergic neurons in a humanized α-synuclein rat model of PD. Proc. Nat. Acad. Sci. U.S.A. 117:15209–15220.

Jash, S., S. Banerjee, M. J. Lee, S. R. Farmer, and V. Puri. 2019. CIDEA transcriptionally regulates UCP1 for britening and thermogenesis in human fat cells. iScience 20:73–89.

Kalashnikov, V., L. Khrabrova, N. Blohina, A. Zaitcev, and T. Kalashnikova. 2020. Dynamics of the inbreeding coefficient and homozygosity in thoroughbred horses in Russia. Animals 10:1217.

Kaviriri, D. K., Q. Zhang, X. Zhang, L. Jiang, J. Zhang, J. Wang, D. P. Khasa, X. You, and X. Zhao. 2020. Phenotypic variability and genetic diversity in a pinus koraiensis clonal trial in Northeastern China. Genes 11:673.

Kijas, J. W., A. P. Gutierrez, R. D. Houston, S. McWilliam, T. P. Bean, K. Soyano, J. E. Symonds, N. King, C. Lind, and P. Kube. 2019. Assessment of genetic diversity and population structure in cultured Australian Pacific oysters. Anim. Genet. 50:686–694.

Kim, E. S., J. B. Cole, H. Huson, G. R. Wiggans, C. P. Van Tassell, B. A. Crooker, G. Liu, Y. Da, and T. S. Sonstegard. 2013. Effect of artificial selection on runs of homozygosity in U.S. Holstein cattle. PLoS One 8:e80813.

Lin, Y. L., Y. W. Lin, J. Nhieu, X. Zhang, and L. N. Wei. 2020. Sonic hedgehog-gli1 signaling and cellular retinoic acid binding protein 1

gene regulation in motor neuron differentiation and diseases. Int. J. Mol. Sci. 21:4125.

Liu, L., C. Liu, M. Zhao, Q. Zhang, Y. Lu, P. Liu, H. Yang, J. Yang, X. Chen, and Y. Yao. 2020. The pharmacodynamic and differential gene expression analysis of PPAR α/δ agonist GFT505 in CDAHFD-induced NASH model. PLoS One 15:e0243911.

Liu, R., M. Zheng, J. Wang, H. Cui, Q. Li, J. Liu, G. Zhao, and J. Wen. 2019. Effects of genomic selection for intramuscular fat content in breast muscle in Chinese local chickens. Anim. Genet. 50:87–91.

López-Cortegano, E., R. Pouso, A. Labrador, A. Pérez-Figueroa, J. Fernández, and A. Caballero. 2019. Optimal management of genetic diversity in subdivided populations. Front. Genet. 10:843.

Madilindi, M. A., C. B. Banga, E. Bhebhe, Y. P. Sanarana, K. S. Nxumalo, M. G. Taela, B. S. Magagula, and N. O. Mapholi. 2020. Genetic diversity and relationships among three Southern African Nguni cattle populations. Trop. Anim. Health Prod. 52:753–762.

Mastrangelo, S., M. Tolone, M. T. Sardina, G. Sottile, A. M. Sutera, R. Di Gerlando, and B. Portolano. 2017. Genome-wide scan for runs of homozygosity identifies potential candidate genes associated with local adaptation in Valle del Belice sheep. Genet. Sel. Evol. 49:84.

Meyermans, R., W. Gorssen, N. Buys, and S. Janssens. 2020. How to study runs of homozygosity using PLINK? A guide for analyzing medium density SNP data in livestock and pet species. BMC Genomics 21:94.

Mukhopadhyay, S., X. Wen, N. Ratti, A. Loktev, L. Rangell, S. J. Scales, and P. K. Jackson. 2013. The ciliary G-protein-coupled receptor Gpr161 negatively regulates the Sonic hedgehog pathway via cAMP signaling. Cell 152:210–223.

Nandolo, W., Y. T. Utsunomiya, G. Mészáros, M. Wurzinger, N. Khayadzadeh, R. B. P. Torrecilha, H. A. Mulindwa, T. N. Gondwe, P. Waldmann, M. Ferenčaković, J. F. Garcia, B. D. Rosen, D. Bickhart, C. P. van Tassell, I. Curik, and J. Sölkner. 2018. Misidentification of runs of homozygosity islands in cattle caused by interference with copy number variation or large intermarker distances. Genet. Sel. Evol. 50:43.

Poplin, R., V. Ruano-Rubio, M. A. DePristo, T. J. Fennell, M. O. Carneiro, G. A. Van der Auwera, D. E. Kling, L. D. Gauthier, A. Levy-Moonshine, D. Roazen, K. Shakir, J. Thibault, S. Chandran, C. Whelan, M. Lek, S. Gabriel, M. J. Daly, B. Neale, D. G. MacArthur, and E. Banks. 2018. Scaling accurate genetic variant discovery to tens of thousands of samples. bioRxiv 201178.

Purcell, S., B. Neale, K. Todd-Brown, L. Thomas, M. A. Ferreira, D. Bender, J. Maller, P. Sklar, P. I. de Bakker, M. J. Daly, and P. C. Sham. 2007. PLINK: a tool set for whole-genome association and population-based linkage analyses. Am. J. Hum. Genet. 81:559–575.

Rodríguez-Ramilo, S. T., M. Baranski, H. Moghadam, H. Grove, S. Lien, M. E. Goddard, T. H. E. Meuwissen, and A. K. Sonesson. 2019. Strong selection pressures maintain divergence on genomic islands in Atlantic cod (Gadus morhua L.) populations. Genetics, selection, evolution: GSE 51:61.

Selvam, R., N. Murali, A. K. Thiruvenkadan, R. Saravanakumar, G. Ponnudurai, and T. P. Jawahar. 2017. Single-nucleotide polymorphism-based genetic diversity analysis of the Kilakarsal and Vembur sheep breeds. Vet. World 10:549–555.

Sharpe, J., L. Lettice, J. Hecksher-Sorensen, M. Fox, R. Hill, and R. Krumlauf. 1999. Identification of sonic hedgehog as a candidate gene responsible for the polydactylous mouse mutant Sasquatch. Curr. Biol. 9:97–100.

Shi, L., L. Wang, J. Liu, T. Deng, H. Yan, L. Zhang, X. Liu, H. Gao, X. Hou, L. Wang, and F. Zhao. 2020. Estimation of inbreeding and identification of regions under heavy selection based on runs of homozygosity in a Large White pig population. J. Anim. Sci. Biotechnol. 11:46.

Smaragdov, M. G., and A. A. Kudinov. 2020. Assessing the power of principal components and wright's fixation index analyzes applied to reveal the genome-wide genetic differences between herds of Holstein cows. BMC Genet. 21:47.

Szmatoła, T., A. Gurgul, I. Jasielczuk, T. Ząbek, K. Ropka-Molik, Z. Litwińczuk, and M. Bugno-Poniewierska. 2019. A comprehensive analysis of runs of homozygosity of eleven cattle breeds representing different production types. Animals 9:1024.

Talebi, R., T. Szmatoła, G. Mészáros, and S. Qanbari. 2020. Runs of homozygosity in modern chicken revealed by sequence data. G3 (Bethesda, Md.) 10:4615–4623.

Tatarinova, T. V., E. Chekalin, Y. Nikolsky, S. Bruskin, D. Chebotarov, K. L. McNally, and N. Alexandrov. 2016. Nucleotide diversity analysis highlights functionally important genomic regions. Sci. Rep. 6:35730.

Wang, X. X., R. J. Luo, B. She, Y. Chen, and J. Guo. 2014. Traditional Chinese medicine (Shun-Qi-Tong-Xie Granule) for irritable bowel syndrome: study protocol for a randomised controlled trial. Trials 15:273.

Wang, Y., F. Song, J. Zhu, S. Zhang, Y. Yang, T. Chen, B. Tang, L. Dong, N. Ding, Q. Zhang, Z. Bai, X. Dong, H. Chen, M. Sun, S. Zhai, Y. Sun, L. Yu, L. Lan, J. Xiao, X. Fang, H. Lei, Z. Zhang, and W. Zhao. 2017. GSA: genome sequence archive. Genomics Proteomics Bioinformat. 15:14–18.

Windig, J. J., M. J. W. Verweij, and J. K. Oldenbroek. 2019. Reducing inbreeding rates with a breeding circle: theory and practice in veluws heideschaap. J. Anim. Breed Genet. 136:51–62.

Xie, R., L. Shi, J. Liu, T. Deng, L. Wang, Y. Liu, and F. Zhao. 2019. Genome-wide scan for runs of homozygosity identifies candidate genes in three pig breeds. Animals 9:518.

Xu, Z., H. Sun, Z. Zhang, Q. Zhao, B. S. Olasege, Q. Li, Y. Yue, P. Ma, X. Zhang, Q. Wang, and Y. Pan. 2019. Assessment of autozygosity derived from runs of homozygosity in jinhua pigs disclosed by sequencing data. Front. Genet. 10:274.

Yang, H. S., J. P. Chhatwal, J. Xu, C. C. White, B. Hanseeuw, J. S. Rabin, K. V. Papp, R. F. Buckley, A. P. Schultz, M. J. Properzi, J. R. Gatchel, R. E. Amariglio, N. J. Donovan, E. C. Mormino, T. Hedden, G. A. Marshall, D. M. Rentz, K. A. Johnson, P. L. De Jager, and R. A. Sperling. 2019. An UNC5C allele predicts cognitive decline and hippocampal atrophy in clinically normal older adults. J. Alzheimers Dis. 68:1161–1170.

Yuan, J., S. Li, Z. Sheng, M. Zhang, X. Liu, Z. Yuan, N. Yang, and J. Chen. 2022. Genome-wide run of homozygosity analysis reveals candidate genomic regions associated with environmental adaptations of Tibetan native chickens. BMC Genomics 23:91.

Zavarez, L. B., Y. T. Utsunomiya, A. S. Carmo, H. H. Neves, R. Carvalheiro, M. Ferenčaković, A. M. Pérez O'Brien, I. Curik, J. B. Cole, C. P. Van Tassell, M. V. da Silva, T. S. Sonstegard, J. Sölkner, and J. F. Garcia. 2015. Assessment of autozygosity in Nellore cows (Bos indicus) through high-density SNP genotypes. Front. Genet. 6:5.

Zhang, C., S. S. Dong, J. Y. Xu, W. M. He, and T. L. Yang. 2019. PopLDdecay: a fast and effective tool for linkage disequilibrium decay analysis based on variant call format files. Bioinformatics 35:1786–1788.

Zhang, J., C. Nie, X. Li, Z. Ning, Y. Chen, Y. Jia, J. Han, L. Wang, X. Lv, W. Yang, and L. Qu. 2020. Genome-wide population genetic analysis of commercial, indigenous, game, and wild chickens using 600K SNP microarray data. Front. Genet. 11:543294.

Zhang, M., W. Han, H. Tang, G. Li, M. Zhang, R. Xu, Y. Liu, T. Yang, W. Li, J. Zou, and K. Wu. 2018. Genomic diversity dynamics in conserved chicken populations are revealed by genome-wide SNPs. BMC Genomics 19:598.

Zhang, Q., M. P. Calus, B. Guldbrandtsen, M. S. Lund, and G. Sahana. 2015. Estimation of inbreeding using pedigree, 50k SNP chip genotypes and full sequence data in three cattle breeds. BMC Genet. 16:88.

Zhang, Z., Y. Sun, W. Du, S. He, M. Liu, and C. Tian. 2017. Effects of vertebral number variations on carcass traits and genotyping of Vertnin candidate gene in Kazakh sheep. Asian-Australas. J. Anim. Sci. 30:1234–1238.